

Vector- and Scalar-Bilepton Pair Production in Hadron Colliders

E. Ramirez Barreto

Centro de Ciências Naturais e Humanas, UFABC
Santo André, SP, Brazil

Y. A. Coutinho

Instituto de Física, UFRJ, Rio de Janeiro, RJ, Brazil

J. Sá Borges

Instituto de Física, UERJ, Rio de Janeiro, RJ, Brazil

Abstract

We study the double-charged vector-bilepton pair production and double-charged scalar-bilepton pair production *via* $p + p \rightarrow Y^{++} + Y^{--} + X$ and $p + p \rightarrow S_1^{++} + S_1^{--} + X$, where Y and S_1 are vector and scalar bileptons respectively, in the framework of the minimal version of the 3-3-1 model. We compute the photon, Z , and Z' s-channel contributions for the elementary process of bilepton scalar pair production, and to keep the correct unitarity behavior for the elementary $q\bar{q}$ interaction, we include the exotic quark t-channel contribution in the vector-bilepton pair production calculation. We explore a mass range for Z' and we fix the exotic quark mass within the experimental bounds. In this model, the vector-bilepton mass is directly related to $M_{Z'}$ and we consider scalar mass values around the vector-bilepton mass.

We show that the total cross section for vector-bilepton production is 3 orders of magnitude larger than for scalar pair production for $\sqrt{s} = 7$ TeV and 14 TeV and we obtain the number of events for the proposed LHC luminosities as a function of the bilepton mass. In addition we present some invariant mass and transverse momentum distributions. When comparing these distributions we observe quite different behavior providing the determination of the bilepton nature. We conclude that one can disentangle the production rates and that the LHC can be capable of detecting these predicted particles as a signal for new physics.

1 Introduction

The standard model (SM) of the strong and the electroweak interactions is a very successful theory and from the present year we expect the confirmation of its main predictions. However it was not tested for $\sqrt{s} > 2$ TeV in hadron colliders, and it is reasonable to ask if nature will present new phenomena not described by the SM. Moreover it is believed that it cannot be the complete theory because it does not explain some theoretical features. This motivates the formulation of many theoretical extensions or alternatives to the SM. These models for physics beyond the SM propose, for example, the existence of new particles and their predictions will be tested at the Large Hadron Collider (LHC) and the International Linear Collider (ILC).

In the SM, the vector bosons and the scalar particles do not carry any leptonic or baryonic quantum number, but some extended models predict vector bosons and/or scalar particles that couple to two leptons. These particles are known as bileptons and their discovery would be a signal of physics beyond the SM. Another signature of new physics can be the presence of an electrically double-charged particle, which can decay, for example, into a same sign lepton pair. Many theoretical models predict particles with these peculiar properties. For example, the doubly charged gauge vector-bilepton bosons are predicted in the $SU(15)$ grand unified theories [1] and also in models with $SU(3)_c \times SU(3)_L \times U(1)_Y$ gauge symmetry, known as the 3-3-1 model [2, 3, 4]. In the left-right symmetric model [5] and in the 3-3-1 model the scalarlike bileptons are in multiplets that are introduced for symmetry breaking purposes. There are composite models, like technicolor [6, 7, 8], that introduce nongauge vector bileptons, and an extension of the SM has fundamental or composite bileptons [9, 10].

In this work, we study the production of bileptons with two units of electric charge and from now on we call them bileptons. They were not observed, but the data extracted from the LEP II experiments can be used to established limits on the vector-bilepton masses around 100 GeV [11]. More exactly, from muonium-antimuonium conversion experiments [12, 13, 14], the upper bound for the ratio of double-charged vector-bilepton-lepton coupling to its mass is of order 0.27 TeV^{-1} with 95% C.L.

In the case of the double-charged scalar-bilepton, CDF and $D\bar{O}$ establish the lower bound for the bilepton mass in the range 110 – 150 GeV [15, 16, 17, 18] with 95% C.L., from the exclusive bilepton decay into left-handed $e\tau$, $\mu\tau$ and

$\mu\mu$ pairs by considering the left-right model, the SM with a Higgs triplet and the little Higgs model.

The study of vector-bilepton pair production from the hadron collider cannot be completely model independent because the SM Drell-Yan process violates unitarity, then requiring extra s - and t -channel contributions from new neutral gauge boson and from exotic fermions [19]. Having this in mind and in order to focus the LHC physics, we do elect a model to get correct unitarity behavior for bilepton pair production in a pp collider. The 3-3-1 model offers the issue for this problem because in its particle content, together with simple and doubly charged vector gauge bileptons, it predicts the existence of an extra neutral gauge boson and exotic fermions whose signatures can be manifest themselves at the early stage of LHC operation. Considering first the gauge sector of the 3-3-1 model, we have explored, in a recent paper, the distributions of dimuons produced at LHC to show a clear signature for the existence of a new neutral gauge boson, called Z' , and compared the invariant mass and angular distributions with those obtained from other models [20]. In another application, by considering the pp collision, we have calculated the production of a pair of single-charged gauge vector bileptons [21], where the cross section correct unitarity behavior follows from the balance between Z' and exotic quark contributions. There is a similar study for bilepton pair production in e^+e^- [22] and a work of the production of just one double-charged vector bilepton [23].

The production of double-charged Higgs was studied in the left-right symmetric model [24] and in the 3-3-1 model with heavy leptons for e^+e^- colliders [25], photon-photon collisions [26], and hadron colliders [27, 28].

Here we compare the production of a pair of gauge bileptons ($Y^{\pm\pm}$) with that of a pair of scalar bilptons ($S_1^{\pm\pm}$) to evaluate the ratio between the production cross sections. Besides this evaluation we also present some distributions that can reveal the signature associated with the vector- or scalarlike nature of the produced pair and we obtain the number of events for $\sqrt{s} = 7$ TeV and 14 TeV at the LHC through the processes $p + p \longrightarrow Y^{++} + Y^{--} + X$ and $p + p \longrightarrow S_1^{++} + S_1^{--} + X$.

In Sec. II we review the basic aspects of the minimal version of the 3-3-1 model. In Sec. III we present the tree level calculation of $q+\bar{q} \longrightarrow Y^{++}+Y^{--}$ and $q+\bar{q} \longrightarrow S_1^{++} + S_1^{--}$ elementary cross sections as well as the final results, adding some comments. Finally, in Sec. IV, we present the conclusions of our work.

2 Model

In the 3-3-1 model the electric charge operator is defined as

$$Q = T_3 + \beta T_8 + XI \quad (1)$$

where T_3 and T_8 are two of the eight generators satisfying the $SU(3)$ algebra

$$[T_i, T_j] = if_{ijk}T_k \quad i, j, k = 1, 2, \dots, 8, \quad (2)$$

I is the unit matrix, and X denotes the $U(1)$ charge.

The electric charge operator determines how the fields are arranged in each representation and depends on the β parameter. Among the possible choices, $\beta = -\sqrt{3}$ [2, 3] corresponds to the minimal version of the model which is used in the present application.

The lepton content of each generation ($a = 1, 2, 3$) is

$$\psi_{aL} = (\nu_a \ell_a \ell_a^c)_L^T \sim (\mathbf{1}, \mathbf{3}, 0), \quad (3)$$

where ℓ_a^c is the charge conjugate of the ℓ_a (e, μ, τ) field. Here the values in the parentheses denote quantum numbers relative to $SU(3)_C$, $SU(3)_L$, and $U(1)_X$ transformations.

The procedure to cancel model anomalies imposes that quark families must be assigned to different $SU(3)$ representation [29]. We elect the left component of the first quark family to be accommodated in $SU(3)_L$ triplet and the second and third families ($m = 2, 3$) to belong to the antitriplet representation, as follows:

$$\begin{aligned} Q_{1L} &= (u_1 \ d_1 \ J_1)_L^T \sim (\mathbf{3}, \mathbf{3}, 2/3) \\ Q_{mL} &= (d_m \ u_m \ j_m)_L^T \sim (\mathbf{3}, \mathbf{3}^*, -1/3) \end{aligned} \quad (4)$$

where $a = 1, 2, 3$ and J_1, j_2 , and j_3 are exotic quarks with, respectively, $5/3$, $-4/3$, and $-4/3$ units of the positron charge (e). We will comment about the consequences of our choice in the conclusion section.

The corresponding right-handed component representations are:

$$\begin{aligned} u_{aR} &\sim (\mathbf{3}, \mathbf{1}, 2/3), \quad d_{aR} \sim (\mathbf{3}, \mathbf{1}, -1/3) \\ J_{1R} &\sim (\mathbf{3}, \mathbf{1}, 5/3), \quad j_{mR} \sim (\mathbf{3}, \mathbf{1}, -4/3) \end{aligned} \quad (5)$$

The gauge bosons come from the combination of nine fields, W_μ^a ($a = 1, 2, \dots, 8$) of $SU(3)_L$ and the $U(1)_X$ B_μ field. We identify the SM W^\pm and four additional charged gauge bosons from the combinations:

$$W_\mu^\pm = \frac{W_\mu^1 \mp i W_\mu^2}{\sqrt{2}}, V_\mu^\pm = \frac{W_\mu^4 \mp i W_\mu^5}{\sqrt{2}}, Y_\mu^{\pm\pm} = \frac{W_\mu^6 \mp i W_\mu^7}{\sqrt{2}},$$

where the new charged bosons carry two units of lepton number and are called bileptons.

In the neutral sector, we define the γ , Z and the new Z' fields:

$$\begin{aligned} A_\mu &= s_W W_\mu^3 - \sqrt{3} s_W W_\mu^8 + \sqrt{1 - 4 s_W^2} B_\mu, \\ Z_\mu &= c_W W_\mu^3 + \sqrt{3} s_W t_W W_\mu^8 - t_W \sqrt{1 - 4 s_W^2} B_\mu, \\ Z'_\mu &= \frac{1}{c_W} \sqrt{1 - 4 s_W^2} W_\mu^8 + \sqrt{3} t_W B_\mu, \end{aligned} \quad (6)$$

where $c_W = \cos \theta_W$, $s_W = \sin \theta_W$, $t_W = s_W/c_W$.

Usually the neutral physical states Z_1 and Z_2 are mixtures of Z and Z' given by

$$Z_1 = \cos \theta_{mix} Z - \sin \theta_{mix} Z', \quad Z_2 = \sin \theta_{mix} Z + \cos \theta_{mix} Z',$$

where, for a small mixing, $\theta_{mix} \ll 1$, Z_2 corresponds to Z' , and Z_1 to Z . The physical and symmetry state masses are related to the mixing angle by

$$\tan^2 \theta_{mix} = \frac{M_Z^2 - M_{Z_1}^2}{M_{Z_2}^2 - M_Z^2}, \quad (7)$$

so for a small mixing angle, M_{Z_1} is close to the SM neutral gauge boson mass and M_{Z_2} to the extra neutral gauge boson one.

There are model dependent experimental bounds for this mixing angle [30]. In the case of the 3-3-1 model, the mixing becomes small for $v_\chi \gg v_\eta, v_\rho, v_{\sigma_2}$ and vanishes if the ρ and the η vacuum expectation values satisfy the relation [31]

$$v_\eta^2 = \frac{1 + 2 s_W^2}{1 - 4 s_W^2} v_\rho^2,$$

independent of the $SU(3)_L$ symmetry breaking scale.

The minimum Higgs structure necessary for symmetry breaking and that gives to quarks acceptable masses is:

$$\eta = \begin{pmatrix} \eta^0 \\ \eta_1^- \\ \eta_2^+ \end{pmatrix} \sim (1, 3, 0), \quad \rho = \begin{pmatrix} \rho^+ \\ \rho^0 \\ \rho^{++} \end{pmatrix} \sim (1, 3, 1), \quad \chi = \begin{pmatrix} \chi^- \\ \chi^{--} \\ \chi^0 \end{pmatrix} \sim (1, 3, -1). \quad (8)$$

To generate the correct lepton mass spectrum, one needs a scalar sextet [32]

$$\Sigma = \begin{pmatrix} \sigma_1^0 & h_2^+ & h_1^- \\ h_2^+ & H_1^{++} & \sigma_2^0 \\ h_1^- & \sigma_2^0 & H_2^{--} \end{pmatrix} \sim (1, 6^*, 0), \quad (9)$$

where in parentheses are, respectively, the dimensions of the group representation of $SU(3)_C$, $SU(3)_L$ and the $U(1)_X$ charges.

The neutral field of each scalar multiplet develops a nonzero vacuum expectation value (v_χ , v_ρ , v_η , and v_{σ_2}) and the breaking of the 3-3-1 group to the SM is produced *via* the following hierarchical pattern:

$$SU_L(3) \otimes U_X(1) \xrightarrow{\langle v_\chi \rangle} SU_L(2) \otimes U_Y(1) \xrightarrow{\langle v_\rho, v_\eta, v_{\sigma_2} \rangle} U_{em}(1).$$

The consistency of the model with the SM phenomenology is imposed by fixing a large scale for v_χ , responsible for giving mass to the exotic particles ($v_\chi \gg v_\rho, v_\eta, v_{\sigma_2}$), with $v_\rho^2 + v_\eta^2 + v_{\sigma_2}^2 = v_W^2 = (246)^2 \text{ GeV}^2$. In the minimal version, the relation between Z' , V , and Y masses [19, 33] is:

$$\frac{M_V}{M_{Z'}} = \frac{M_Y}{M_{Z'}} = \frac{\sqrt{3 - 12s_w^2}}{2c_w}. \quad (10)$$

This constraint respects the experimental bounds, and is a consequence of the model, but it is not often used in the literature. We keep this relation through our calculations. This ratio is $\simeq 0.3$ for $s_w = 0.23$ [30], and so, in this minimal version of the model, Z' can decay into a bilepton pair.

The relation between the $SU_L(3)$ and $U_X(1)$ couplings for the minimal version of the model is

$$\frac{g'^2}{g^2} = \frac{\sin^2 \theta_w}{1 - 4 \sin^2 \theta_w}, \quad (11)$$

which fixes $\sin^2 \theta_w < 1/4$, which is a peculiar characteristic of the minimal version of the 3-3-1 model.

The coupling between the gauge bosons and the scalar bosons comes from the gauge invariant kinetic-energy term in the Lagrangian:

$$\mathcal{L}_\varphi^{min} = \text{Tr} \left((D_\mu \varphi)^\dagger (D_\mu \varphi) \right) + V(\varphi), \quad (12)$$

where $\varphi = \eta, \rho, \chi$ and Σ . The covariant derivative of the triplet $\varphi = \eta, \rho, \chi$ is

$$\mathcal{D}_\mu \varphi = \partial_\mu \varphi - i \frac{g}{2} \mathcal{M}_\mu \varphi - i g_X X_\varphi B_\mu \varphi. \quad (13)$$

The covariant derivative of the sextet is

$$\mathcal{D}_\mu \Sigma = \partial_\mu \Sigma - i \frac{g}{2} \left[\mathcal{M}_\mu \Sigma + \Sigma^T \mathcal{M}_\mu^T \right] - i g_X X_\Sigma B_\mu \Sigma, \quad (14)$$

with \mathcal{M}_μ defined as

$$\mathcal{M}_\mu = \begin{pmatrix} W_\mu^3 + \frac{1}{\sqrt{3}} W_\mu^8 & \sqrt{2} W_\mu^+ & \sqrt{2} V_\mu^- \\ \sqrt{2} W_\mu^- & W_\mu^3 - \frac{1}{\sqrt{3}} W_\mu^8 & \sqrt{2} Y_\mu^{--} \\ \sqrt{2} V_\mu^+ & \sqrt{2} Y_\mu^{++} & -\frac{2}{\sqrt{3}} W_\mu^8 \end{pmatrix}. \quad (15)$$

and X_φ and X_Σ are the triplet and sextet $U(1)_X$ charges.

The symmetry breaking leads to a shift on the neutral scalar fields, and as a consequence, the physical states are related to the symmetry states. From the more general potential proposed in [34], which involves all triplets and the sextet, we select the terms where the double-charged scalars ($H_1^{++}, H_2^{++}, \rho^{++}$, and χ^{++}) are mixed together. From a convenient approximation for the parameters of the double-charged scalar mass matrix we can identify χ^{++} as a Goldstone state (to be eaten by Y^{++}). The χ^{++} decoupling leads to three massive states, the physical state $S_1^{++} \sim H_1^{++}$ and two physical states from the mixing between ρ^{++} and H_2^{++} .

The Lagrangian for the coupling of the sextet to each lepton family is given by

$$\mathcal{L}_\Sigma = -\frac{1}{2} \sum_{i,j=1}^3 G_{ij} \bar{\ell}_L^i (\ell_L^j)^c \Sigma^{ij} + H. c.; \quad (16)$$

in particular the interactions involving the double-charged scalar $H_1^{++} \sim S_1^{++}$ are obtained from:

$$\mathcal{L}_{S_1} = -\frac{1}{2} G_{\ell\ell} \bar{\ell}_R^c \ell_L S_1^{++} + H. c., \quad \ell = e, \mu, \tau, \quad (17)$$

where $G_{\ell\ell} = m_\ell/v_{\sigma_2}$.

We decide to study this scalar particle production because its main decay mode is into two τ giving a clear signature for its existence. The total $S_1^{\pm\pm}$ width is 2×10^{-2} , 2.7×10^{-2} , 4×10^{-2} , and 11×10^{-2} GeV for $M_{S_1} = 150$, 200, 300, and 400 GeV, by fixing $v_{\sigma_2} = 123$ GeV [34].

The trilinear gauge couplings (TGC) in this model are obtained from the part of the Lagrangian describing the self-interactions of gauge fields:

$$\mathcal{L}_{TGC} = -g f_{abc} \partial_\mu W_\nu^a W^{b\mu} W^{c\nu}, \quad a, b, c = 1, 2, \dots, 8, \quad (18)$$

where f_{abc} is the $SU(3)$ antisymmetric structure constant.

Expressing W^a ($a = 1, 2, \dots, 8$) in terms of the neutral and double-charged physical fields, a straightforward calculation leads to

$$\begin{aligned} \mathcal{L}_{TGC}^{min} = & -2ig s_w [A^\nu (Y_{\mu\nu}^{--} Y^{++\mu} - Y_{\mu\nu}^{++} Y^{--\mu}) + A_{\mu\nu} Y^{--\mu} Y^{++\nu}] \\ & -ig \frac{1-4s_w^2}{2c_w} [Z^\nu (Y_{\mu\nu}^{--} Y^{++\mu} - Y_{\mu\nu}^{++} Y^{--\mu}) + Z_{\mu\nu} Y^{--\mu} Y^{++\nu}] \\ & +ig \frac{\sqrt{3-12s_w^2}}{2c_w} [Z'^\nu (Y_{\mu\nu}^{--} Y^{++\mu} - Y_{\mu\nu}^{++} Y^{--\mu}) + Z'_{\mu\nu} Y^{--\mu} Y^{++\nu}] \end{aligned} \quad (19)$$

where $Y_{\mu\nu} \equiv \partial_\mu Y_\nu - \partial_\nu Y_\mu$. The trilinear couplings used in this paper are shown in Table I. We obtain, from the expressions (13) and (14), the couplings between the gauge boson and the double-charged scalar S_1^{++} shown in Table II. The charged current interaction of leptons with the vector bilepton is given by

$$\mathcal{L}^{CC} = -\frac{g}{\sqrt{2}} (\ell^T C \gamma^\mu \gamma^5 \ell Y_\mu^{++}) + H. c., \quad (20)$$

where C is the charge conjugation matrix.

This double-charged bilepton decays into a pair of equal charged leptons with the same width. They are 1.8, 2.3, and 2.8 GeV for $M_Y = 214$, 271, and 325 GeV, respectively.

In the neutral gauge sector, the interactions of fermions Ψ_f and bosons are described by the Lagrangian:

$$\begin{aligned} \mathcal{L}_{NC} = & \sum_f eq_f \bar{\Psi}_f \gamma^\mu \Psi_f A_\mu - \frac{g}{2c_w} \{ \bar{\Psi}_f \gamma^\mu (g_{V_f} - g_{A_f} \gamma^5) \Psi_f Z_\mu \\ & + \bar{\Psi}_f \gamma^\mu (g'_{V_f} - g'_{A_i} \gamma^5) \Psi_f Z'_\mu \}, \end{aligned} \quad (21)$$

where $e q_f$ is the fermion electric charge and g_{V_f} , g_{A_f} , g'_{V_f} , and g'_{A_f} are the fermion vector and axial-vector couplings with Z and Z' , respectively.

As referred to before, in the 3-3-1 model one quark family must transform with respect to $SU(3)$ rotations differently from the other two. This requirement manifests itself when we collect the quark currents in a part with universal coupling to Z' similar to the SM and another part corresponding to the nondiagonal Z' coupling. The transformation of these nondiagonal terms, in the mass eigenstates basis, leads to the flavor changing neutral Lagrangian

$$\mathcal{L}_{FCNC} = \frac{g c_w}{\sqrt{3 - 12s_w^2}} \left(\bar{U}_L \gamma^\mu \mathcal{U}_L^\dagger B \mathcal{U}_L U_L + \bar{D}_L \gamma^\mu \mathcal{V}_L^\dagger B \mathcal{V}_L D_L \right) Z'_\mu. \quad (22)$$

where

$$U_L = (u \ c \ t)_L^T, \quad D_L = (d \ s \ b)_L^T \quad \text{and} \quad B = \text{diag} (1 \ 0 \ 0).$$

The mixing matrices \mathcal{U} (for up -type quark) and \mathcal{V} (for $down$ -type quark) come from the Yukawa Lagrangian and are constrained by the Cabibbo-Kobayashi-Maskawa matrix, as

$$\mathcal{U}^\dagger \mathcal{V} = V_{CKM}. \quad (23)$$

By convention in the SM up -type quark gauge eigenstates are the same as the mass eigenstates, which corresponds to $\mathcal{U} = I$. This assumption is not valid in the 3-3-1 model because, in accordance to the renormalization group equations, all matrix elements evolve with energy and are unstable against radiative corrections, and then \mathcal{U} must be $\neq I$. As the Eq. (23) is independent of representation, one is free to choose which quark family representation must be different from the other two. We recall that here the first family belongs to the $SU(3)$ triplet representation. In the next section we will discuss the consequences of our choice.

All universal neutral couplings diagonal and nondiagonal are presented in Tables III and IV, respectively.

The couplings of ordinary to exotic quarks are driven by the double-charged bilepton as follows:

$$\mathcal{L}_{CC} = -\frac{g}{2\sqrt{2}} [\bar{u} \gamma^\mu (1 - \gamma^5) (\mathcal{U}_{21} J_2 + \mathcal{U}_{31} J_3) + \bar{J}_1 \gamma^\mu (1 - \gamma^5) \mathcal{V}_{11} d] Y_\mu^{++}. \quad (24)$$

where \mathcal{U}_{21} , \mathcal{U}_{31} , and \mathcal{V}_{11} are mixing matrices elements [Eq. (22)]. From this expression and considering the conservation of the leptonic number, we

Vertex	$\gamma Y^{++}Y^{--}$	$ZY^{++}Y^{--}$	$Z'Y^{++}Y^{--}$
Coupling	$2e$	$e \frac{1 - 4 s_w^2}{2 s_w c_w}$	$-\frac{e}{2 s_w c_w} \sqrt{3 - 12 s_w^2}$

Table 1: Couplings of neutral gauge bosons with vector-bilepton $Y^{\pm\pm}$.

Vertex	$\gamma S_1^{++}S_1^{--}$	$ZS_1^{++}S_1^{--}$	$Z'S_1^{++}S_1^{--}$
Coupling	$2e$	$\frac{g(1 - 2 s_w^2)}{c_w}$	$\frac{g(1 - 4 s_w^2)}{6 c_w}$

Table 2: Couplings of neutral gauge bosons with scalar-bilepton $S_1^{\pm\pm}$.

conclude that the exotic quarks carry two units of leptonic quantum number and so they are a class of leptoquarks.

	Vector couplings	Axial-vector couplings
$Z\bar{u}_i u_i$	$\frac{1}{2} - \frac{4s_w^2}{3}$	$\frac{1}{2}$
$Z\bar{d}_j d_j$	$-\frac{1}{2} + \frac{2s_w^2}{3}$	$-\frac{1}{2}$
$Z'\bar{u}_i u_i$	$\frac{1 - 6s_w^2 - \mathcal{U}_{ii}^* \mathcal{U}_{ii} c_w^2}{2\sqrt{3} - 12s_w^2}$	$\frac{1 + 2s_w^2 + \mathcal{U}_{ii}^* \mathcal{U}_{ii} c_w^2}{2\sqrt{3} - 12s_w^2}$
$Z'\bar{d}_j d_j$	$\frac{1 - \mathcal{V}_{jj}^* \mathcal{V}_{jj} c_w^2}{2\sqrt{3} - 12s_w^2}$	$\frac{1 - 4s_w^2 + \mathcal{V}_{jj}^* \mathcal{V}_{jj} c_w^2}{2\sqrt{3} - 12s_w^2}$

Table 3: The Z and Z' vector and axial-vector couplings to quarks ($u_1 = u, u_2 = c, u_3 = t$, and $d_1 = d, d_2 = s, d_3 = b$) in the minimal model and \mathcal{U}_{ii} and \mathcal{V}_{jj} are \mathcal{U} and \mathcal{V} diagonal mixing matrix elements.

3 Results

In this paper we investigate the $SU(3)$ vector-bilepton ($Y^{\pm\pm}$) pair production and the scalar-bilepton ($S_1^{\pm\pm}$) pair production in the pp collision at LHC. The physical scalar-bilepton states emerge from the symmetry breaking mechanism which evolves triplets as well as scalar sextet from the Higgs sector of the minimal version of the 3-3-1 model. In our calculation the bilepton mass is related to the mass of the extra neutral gauge boson Z' , also predicted in the model, by Eq. (10). For the Z' mass we adopt some values in accordance with accepted bounds [30]: $M_{Z'}=800, 1000$, and 1200 GeV resulting in $M_{Y^{\pm\pm}} = 214$ GeV, 271, GeV and 325 GeV, respectively. The corresponding Z' widths are 146 GeV, 180 GeV, and 218 GeV.

Using the LEP precision measurements data and considering the contribution of the vector bileptons of the 3-3-1 model in the calculation of the corrections to $Z \rightarrow \bar{b}b$ decay, one determines the allowed region for the bilepton mass

as a function of the exotic quark mass, M_Q . In our calculation we consider $M_Q = 600$ GeV, respecting the experimental bounds [35, 36, 37] and leading to M_Y from 180 to 500 GeV [38].

We consider the elementary process, $q_i + \bar{q}_i \longrightarrow Y^{++} + Y^{--}$ ($q_i = u, d$), taking into account all contributions: γ , Z , and Z' in the s channel and exotic heavy quark contributions in the t channel. For the scalar pair production in $q_i + \bar{q}_i \longrightarrow S_1^{++} + S_1^{--}$ ($q_i = u, d$) there are only γ , Z , and Z' s -channel contributions. We do not consider gluon fusion contributions which were shown to be negligible [28]. We perform the amplitude algebraic calculation with FORM [39], and the details are presented in the paper [21].

Let us consider $\sqrt{s} = 7$ TeV. The results shown in Fig. 1 for vector-bilepton pair production correspond to the quark mixing parameters: $\mathcal{U}_{21} = 0.0054$, $\mathcal{U}_{31} = 0.7662$, and $\mathcal{V}_{11} = 0.8667$. we can note the good behavior of the elementary cross sections that present a peak around the Z' mass and become broader and smaller as the Z' mass increase.

For the analysis of the elementary cross section for scalar-bilepton pair production we consider $M_{S_1} = 200$ GeV and 400 GeV. In Fig. 2 ($M_{Z'} > 2M_{S_1}$) we observe two peaks due to s -channel interference, which are more clear for the subprocess $\bar{d}d$; one peak is associated to the pair production threshold and another one is near $M_{Z'}$. In Fig. 3 ($M_{Z'} \simeq 2M_{S_1}$) the second peak disappears, and as expected, the increase of the bilepton mass reduces the elementary cross section value.

Next we show our results for the bilepton pair production cross section in pp collisions obtained by integrating the elementary cross section weighted by the distribution function for partons in the proton [40] and applying a cut on the pseudorapidity of the final bileptons $|\eta| \leq 3$ as well as a cut on the final transverse momentum $p_t > 20$ GeV.

As shown in Fig. 4, the Z' mass dependent cross section for vector-bilepton pair production is about 3 orders of magnitude larger than the almost constant scalar-bilepton pair production. In contrast with the vector coupling, the scalar- Z' coupling does not depend on the Z' mass.

Let us consider the invariant mass and transverse momentum distributions. First, for $p + p \longrightarrow S_1^{++} + S_1^{--} + X$, we present the invariant mass and transverse momentum distributions in Fig. 5 for three values of the Z' mass and $M_{S_1} = 200$ GeV. In the invariant mass distribution we find a broad peak corresponding to the Z' mass while in the transverse momentum distribution this shape appears close to $M_{Z'}/2$.

In Fig. 6 we display the comparison between the normalized transverse

momentum distributions by fixing $M_Y = 271$ GeV and $M_{S_1} = 200$ GeV. We note different shapes: the vector bileptons are mainly produced with high transverse momenta while the scalar pair production occurs at lower momenta. This is also a nice signature to distinguish the bilepton nature. On the other hand, the normalized scalar and vector rapidity distributions are flat and similar and so they do not allow one to disentangle the produced particles.

To complete our analysis we consider $\sqrt{s} = 14$ TeV for $M_{Z'} = 1000$ GeV. In Fig. 7 we display the comparison between the Z' dependent total cross sections and we realize that the vector-bilepton pair production is again about 3 orders of magnitude larger than for a pair of scalars.

Next we compare, in Fig. 8, the normalized invariant mass distribution for $M_Y = 271$ GeV and for two values of the S_1 mass (150 and 300 GeV). We observe that the distributions are quite different: for the vector bilepton just one peak appears at $M_{Z'}$, whereas, for the scalar one, there is another enhancement for the small scalar-bilepton mass pair.

In Fig. 9, the transverse momentum distributions show that it is possible to disentangle the produced bileptons: exactly as for $\sqrt{s} = 7$ TeV, one vector bilepton is produced with higher momentum than one of the scalar bilepton. We show, in Fig. 10, the number of events as a function of the bilepton mass. The expected number of vector-bilepton pairs produced by year is in the range 10^2 to 10^4 for $\sqrt{s} = 7$ TeV and 10^5 to 10^6 for 14 TeV, corresponding to 1 and 100 fb^{-1} integrated luminosities, respectively. The expected number of scalar-bilepton pairs is about 3 orders of magnitude smaller.

Finally we explore the consequences of $Z - Z'$ mixing, expressed by Eq. (7). The data extracted from LEP, SLC and Tevatron experiments indicate a range $-1.3 \times 10^{-3} \leq \theta_{mix} \leq 0.6 \times 10^{-3}$ for the left-right symmetric model and $-1.6 \times 10^{-3} \leq \theta_{mix} \leq 0.6 \times 10^{-3}$ for the E_χ model [30]. We present the explicit dependence of the bilepton production cross section with the mixing angle for the minimal version of the 3-3-1 model, used in this work. In order to do that, we adopt very large values for this parameter and we show in the Fig. 11 (top and bottom) our findings. First, for vector-bilepton production, we do not observe any dependence on θ_{mix} for $\sqrt{s} = 7$ TeV and $\sqrt{s} = 14$ TeV. Next, for the production of scalars, we note a weak dependence on θ_{mix} when this mixing is completely out of the expected experimental window. On the other hand, as the 3-3-1 model reproduces the low energy SM phenomenology, we assume that it cannot modify substantially, for instance, the ρ parameter. As shown in [41], the precision electroweak data strongly constrain the Z - Z'

mixing angle at low energy. We expect that this conclusion is also valid for the present model, and so we do not introduce any $Z - Z'$ mixing in our calculation.

4 Conclusions

In this paper we focus on the scalar- and vector-bilepton pair production in the pp collision at LHC. These particles are predicted in some extensions of the SM and, in particular, in the 3-3-1 model used in the present paper. For the elementary Drell-Yan process we consider the contributions of γ , Z , and Z' in the s channel for the scalars' production, whereas for the vector-bilepton pair production we add the t-channel exchange of the exotic quarks J_1 , j_2 , and j_3 . We do not consider the very small gluon fusion contribution to these processes.

We take into account the mixing of t-channel quark mass eigenstates originating from the Yukawa coupling, and obtain a set of mixing parameters allowing for good behavior of the elementary cross section. The resulting parameters are related to our particular choice for $SU(3)_L$ family representation. This result does not exclude any other choice for quark representation.

We show that the cross section for vector pair production is about 3 orders of magnitude larger than that for scalar S_1 . To reinforce the possibility to determine the nature of the produced bilepton, we obtain normalized invariant mass and transverse momentum distributions shown in Figs. 9 and 10.

Let us mention that the production of this doubly charged scalar bilepton was not yet studied in the literature; however, there is an application of the 3-3-1 model with heavy leptons which consider the production of a double-charged Higgs belonging to a triplet $SU(3)_L$ representation, with different decay channels. We recall that the scalar considered here decays mainly into a pair of τ leptons, leading to a very clear signature when compared with that from the background corresponding to two Z , two W , or one Z .

We also show the very small dependence of the total cross section on $Z - Z'$ mixing. We are sure that no mixing is to be considered in our calculation motivated by the experimental results from LEP, SLC, and Tevatron and the low energy electroweak precision data that suggest a very small mixing.

Finally, from the expected number of events we conclude that it is possible to confirm the very existence of a new physics at the first stage of the LHC

operation.

Acknowledgments: E. Ramirez Barreto thanks Capes-PNPD. J. Sá Borges and Y. A. Coutinho thank FAPERJ for financial support.

References

- [1] P. H. Frampton and B. -H. Lee, Phys. Rev. Lett. **64**, 619 (1990).
- [2] F. Pisano and V. Pleitez, Phys. Rev. D **46**, 410 (1992).
- [3] P. H. Frampton, Phys. Rev. Lett. **69**, 2889 (1992).
- [4] J. E. Cieza Montalvo, M. D. Tonasse, Phys. Rev. D **67**, 075022 (2003).
- [5] An extensive list of references can be found in R. N. Mohapatra and P. B. Pal, "Massive Neutrinos in Physics and Astrophysics", World Scientific, Singapore, 1998.
- [6] G. G. Ross, "Grand Unified Theories", (1985) Benjamin-Cummins, Menlo Park.
- [7] E. Fahri, L. Susskind, Phys. Rep. **74**, 277 (1981).
- [8] E. Eichten *et al.* , Rev. Mod. Phys. **56** 579 (1984).
- [9] H. Georgi, M. Machacek, Nucl. Phys. B **262**, 463 (1985).
- [10] J. F. Gunion, R. Vega, J. Wudka, Phys. Rev. D **42**, 1673 (1990).
- [11] E. M. Gregores, A. Gusso, S. F. Novaes, Phys. Rev. D **64**, 015004 (2001).
- [12] L. Willmann *et al.* , Phys. Rev. Lett. **82**, 49 (1999).
- [13] H. Fujii, Y. Mimura, K. Sasaki and T. Sasaki, Phys. Rev. D **49**, 559 (1994).
- [14] D. Chang, W.-Y. Keung, Phys. Rev. Lett. **62**, 2583 (1989).
- [15] D. E. Costa *et al.*, Phys. Rev. Lett. **93**, 221802 (2004).

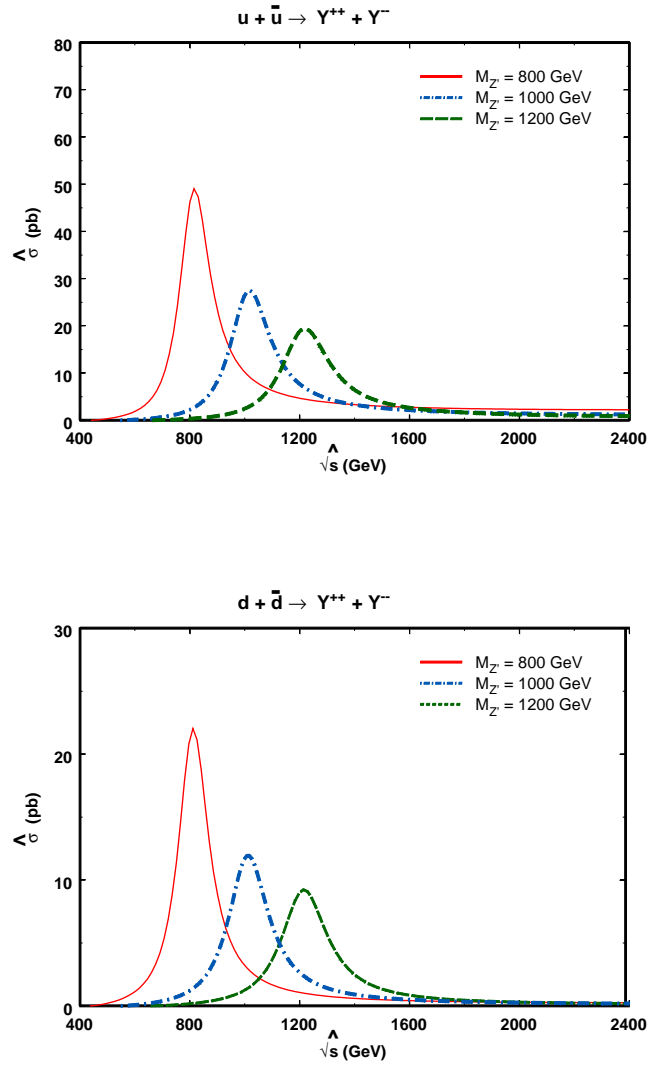


Figure 1: The cross section for the elementary process $u + \bar{u} \rightarrow Y^{++} + Y^{--}$ (top) and $d + \bar{d} \rightarrow Y^{++} + Y^{--}$ (bottom) for $M_{Z'} = 800$ GeV, 1000 GeV, and 1200 GeV.

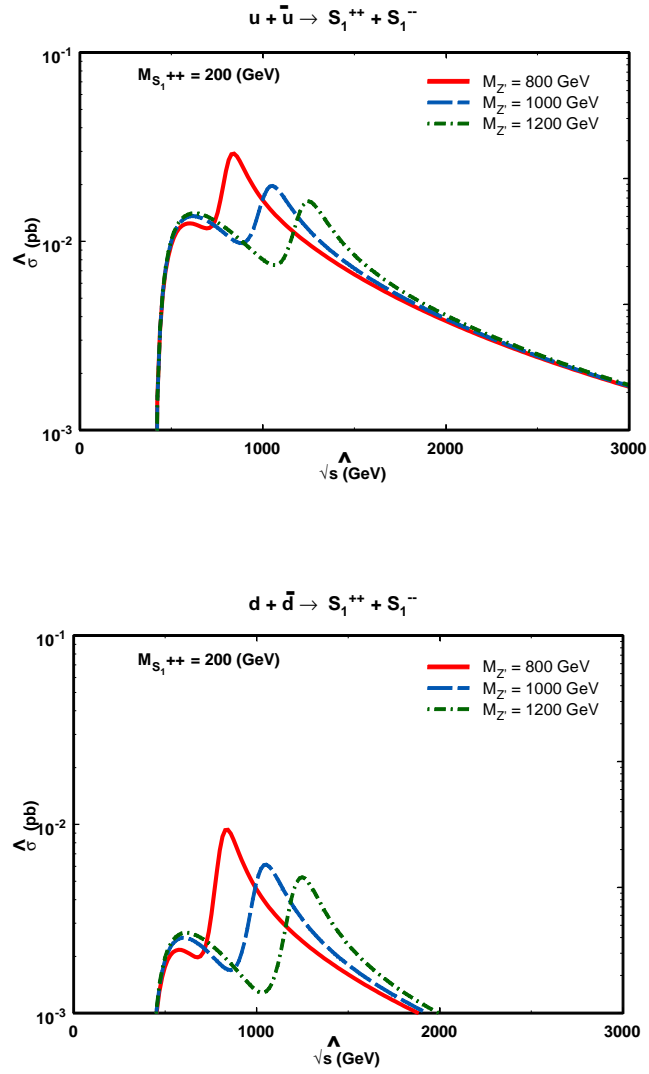


Figure 2: The cross section for the elementary process $u + \bar{u} \rightarrow S_1^{++} + S_1^{-}$ (top) and $d + \bar{d} \rightarrow S_1^{++} + S_1^{-}$ (bottom) for $M_{Z'} = 800 \text{ GeV}$, 1000 GeV , and 1200 GeV and $M_{S_1} = 200 \text{ GeV}$.

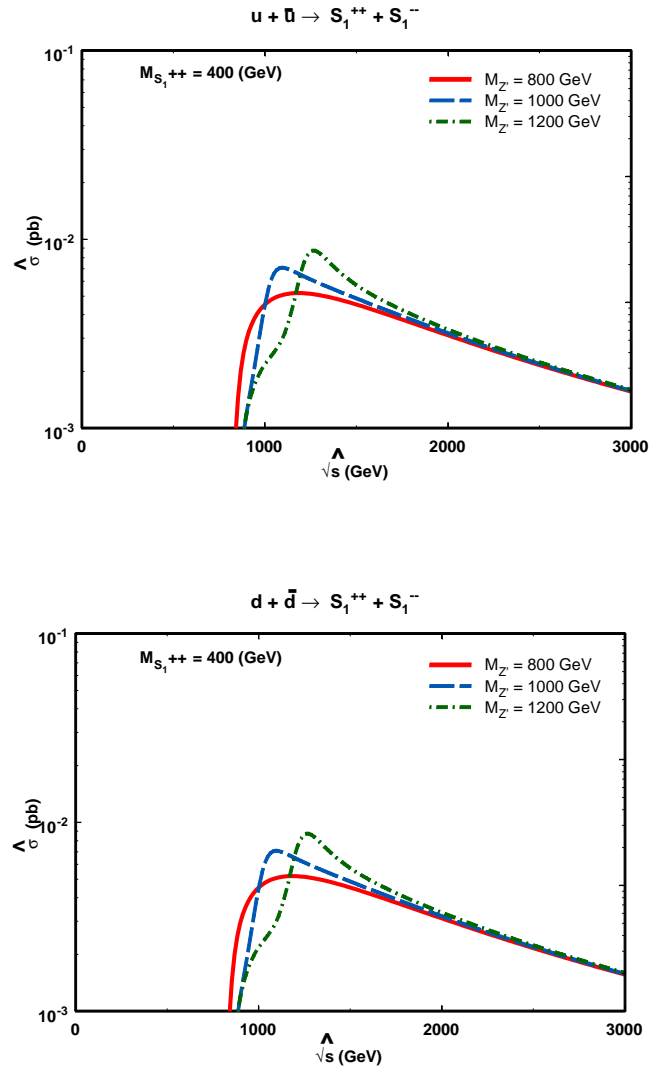


Figure 3: The cross section for the elementary process $u + \bar{u} \rightarrow S_1^{++} + S_1^{--}$ (top) and $d + \bar{d} \rightarrow S_1^{++} + S_1^{--}$ (bottom) for $M_{Z'} = 800$ GeV, 1000 GeV, and 1200 GeV and $M_{S_1} = 400$ GeV.

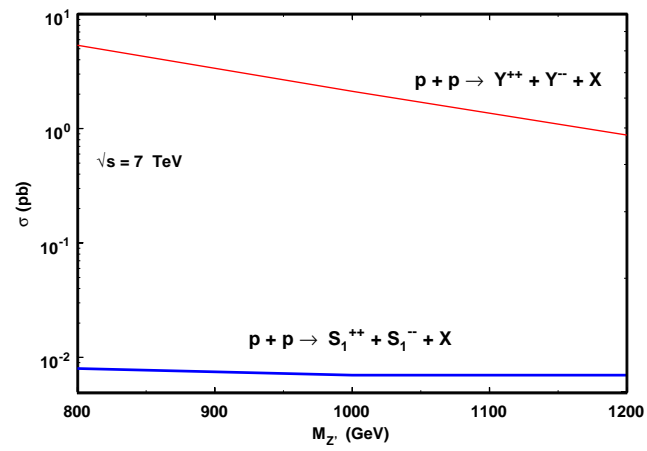


Figure 4: The total cross section for the processes $p + p \rightarrow Y^{++} + Y^{--} + X$ (blue solid line) and $p + p \rightarrow S_1^{++} + S_1^{--} + X$ (red dashed line) for $\sqrt{s} = 7$ TeV.

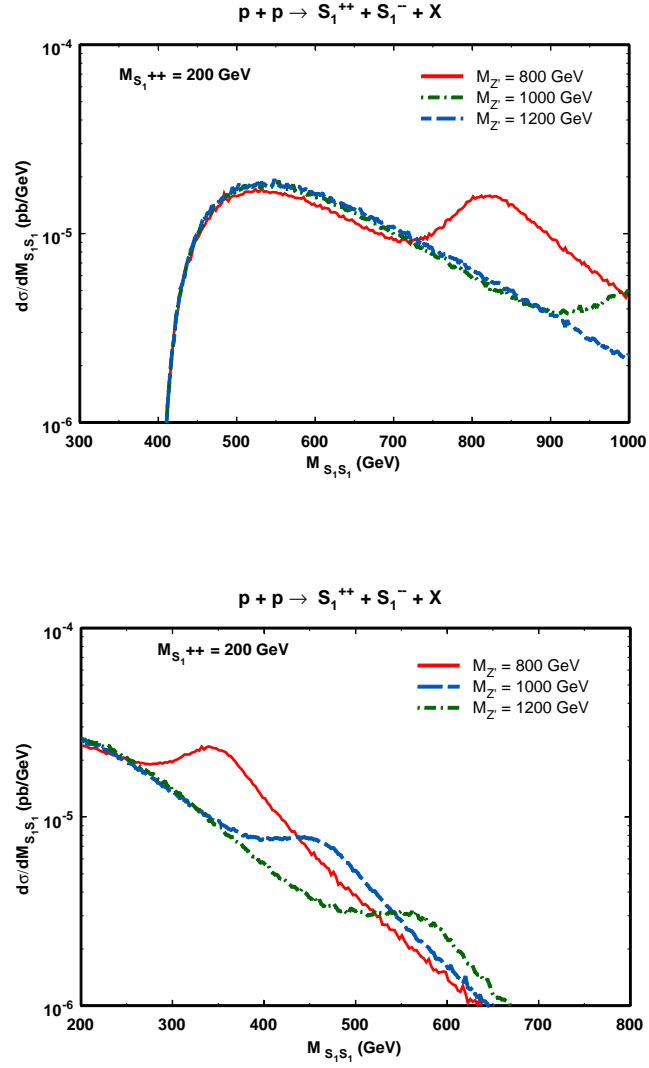


Figure 5: The invariant mass distribution for the process $p + p \rightarrow S_1^{++} + S_1^{-} + X$ (top) and the momentum transverse distribution (bottom) for $M_{Z'} = 800$ GeV, 1000 GeV, and 1200 GeV and $M_{S_1} = 200$ GeV and for $\sqrt{s} = 7$ TeV.

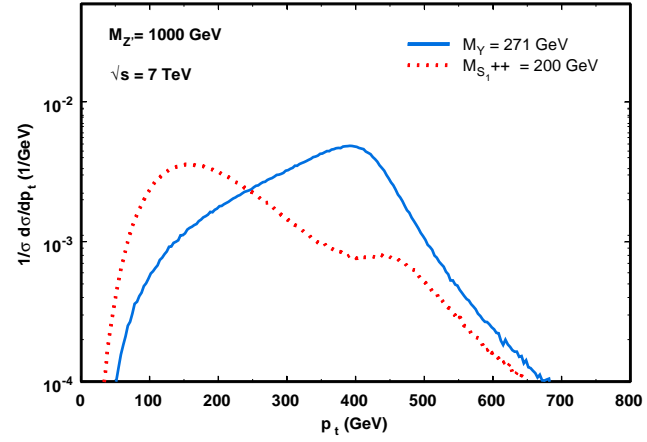
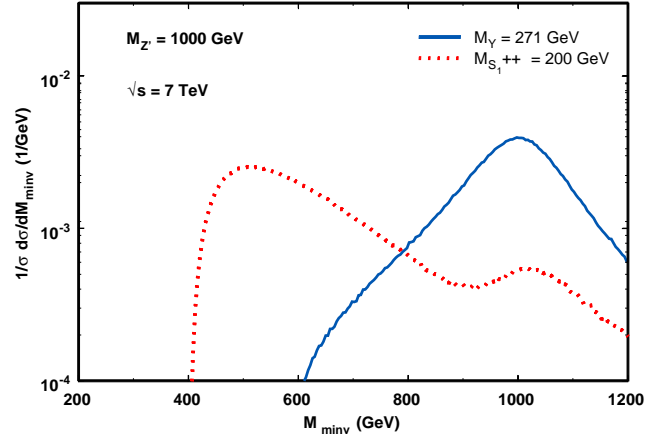


Figure 6: The normalized invariant mass distribution (top) and normalized momentum transverse distribution (bottom) for $\sqrt{s} = 7 \text{ TeV}$.

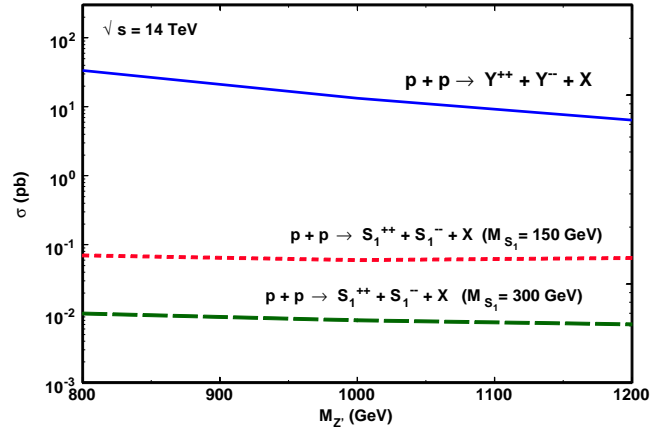


Figure 7: The total cross section for $p + p \rightarrow Y^{++} + Y^{--} + X$ (blue solid line) and $p + p \rightarrow S_1^{++} + S_1^{--} + X$ (red short-dashed and green long-dashed line) as a function of $M_{Z'}$ ($\sqrt{s} = 14$ TeV).

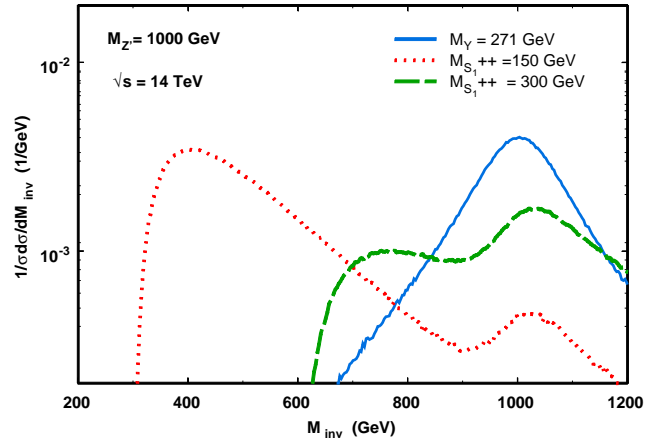


Figure 8: The normalized invariant mass distribution for $p + p \longrightarrow Y^{++} + Y^{--} + X$ and $p + p \longrightarrow S_1^{++} + S_1^{--} + X$ ($\sqrt{s} = 14 \text{ TeV}$).

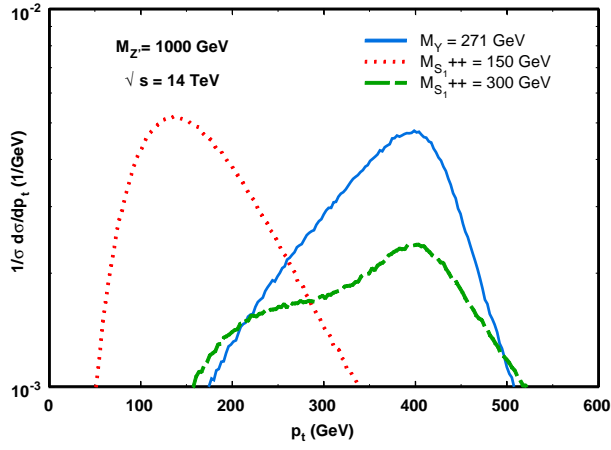


Figure 9: The normalized momentum transverse distribution for $p + p \rightarrow Y^{++} + Y^{--} + X$ and $p + p \rightarrow S_1^{++} + S_1^{--} + X$ ($\sqrt{s} = 14 \text{ TeV}$).

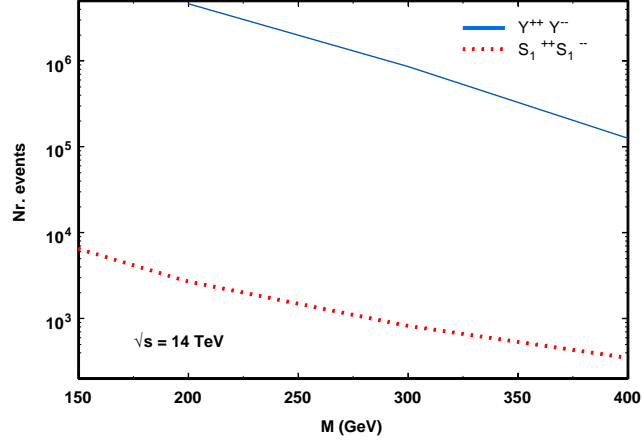
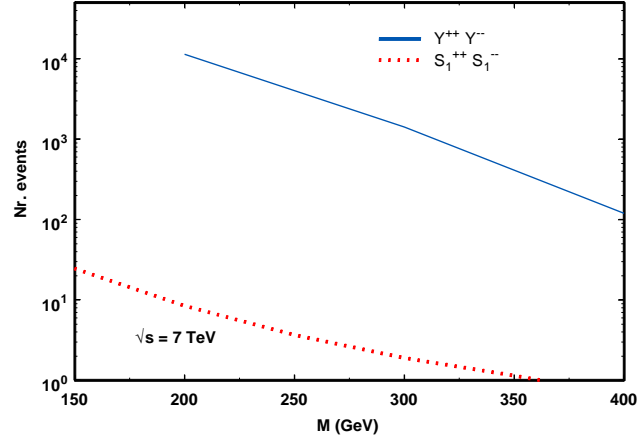


Figure 10: Number of events for $p + p \longrightarrow Y^{++} + Y^{--} + X$ (blue solid line) and $p + p \longrightarrow S_1^{++} + S_1^{--} + X$ (red dotted line) as a function of the bilepton mass. For $\sqrt{s} = 7 \text{ TeV}$ ($\mathcal{L} = 1 \text{ fb}^{-1}$) (top) and $\sqrt{s} = 14 \text{ TeV}$ ($\mathcal{L} = 100 \text{ fb}^{-1}$) (bottom).

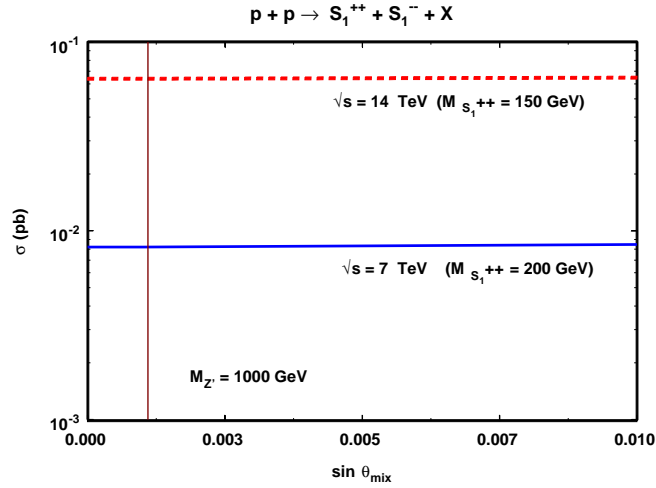
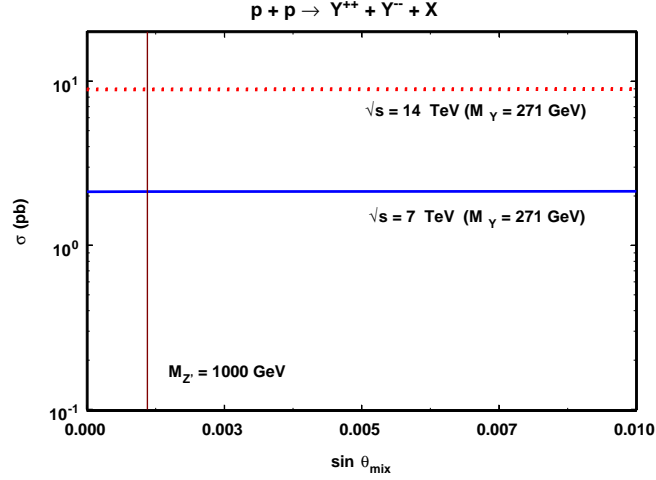


Figure 11: The total cross section for $p + p \rightarrow Y^{++} + Y^{-} + X$ as a function of $\sin \theta_{mix}$ (top). The total cross section for $p + p \rightarrow S_1^{++} + S_1^{-} + X$ as a function of $\sin \theta_{mix}$ (bottom). Both cross sections were calculated for $\sqrt{s} = 7$ TeV and $\sqrt{s} = 14$ TeV. The vertical red line represents the experimental upper bound on $\sin \theta_{mix}$.

- [16] V. M. Abazov *et al.*, Phys. Rev. Lett. **93**, 141801 (2004).
- [17] V. M. Abazov *et al.*, Phys. Rev. Lett. **101**, 071803 (2008).
- [18] T. Aaltonen *et al.*, Phys. Rev. Lett. **101**, 121801 (2008).
- [19] B. Dion, T. Grégoire, D. London, L. Marleau, and H. Nadeau, Phys. Rev. D **59**, 075006 (1999).
- [20] E. Ramirez Barreto, Y. A. Coutinho, J. Sá Borges, Phys. Lett. B **689**, 36 (2010).
- [21] E. Ramirez Barreto, Y. A. Coutinho, J. Sá Borges, Nucl. Phys. B **810**, 210 (2009).
- [22] Hoang Ngoc Long, Dang Van Soa, Nucl. Phys. B **601**, 361 (2001).
- [23] B. Dutta, S. Nandi, Phys. Lett. B **340**, 86 (1994).
- [24] T. Rizzo, Phys. Rev. D **25**, 1355 (1982).
- [25] J. E. Cieza Montalvo, Nelson V. Cortez, M. D. Tonasse, Phys. Rev. D **78**, 116003 (2008).
- [26] J. E. Cieza Montalvo, Nelson V. Cortez, M. D. Tonasse, Phys. Rev. D **77**, 095015 (2008).
- [27] J. E. Cieza Montalvo, Nelson V. Cortez, M. D. Tonasse, Phys. Rev. D **76**, 117703 (2007).
- [28] J. E. Cieza Montalvo, Nelson V. Cortez, M. D. Tonasse, Nucl. Phys. B **756**, 1 (2006), *Erratum-ibid* B **796**, 422(2008).
- [29] A. Carcamo, R. Martinez, and F. Ochoa, Phys. Rev. D **73**, 035007 (2006).
- [30] K. Nakamura *et al.* (Particle Data Group) J. Phys. G **37**, 075021 (2010).
- [31] Phung Van Dong, Hoang Ngoc Long, Eur. Phys. J C **42**, 325 (2005); Alex G. Dias, J. C. Montero and V. Pleitez, Phys. Rev. D **73**, 113004 (2006).

- [32] R. Foot, O. F. Hernandez, F. Pisano, V. Pleitez, Phys. Rev. D **47**, 4158 (1993).
- [33] Daniel Ng, Phys. Rev. D **49**, 4805 (1994).
- [34] Nguen Tuan Anh, Nguen Anh Ky and Honag Ngoc Long, Int. J. Mod. Phys. A **16**, 541 (2001).
- [35] V. M. Abazov *et al.*, Phys. Lett. B **681**, 224 (2009).
- [36] V. M. Abazov *et al.*, Phys. Lett. B **671**, 224 (2009).
- [37] V. M. Abazov *et al.*, Phys. Rev. Lett. **101**, 241802 (2008).
- [38] G. A. González-Sprinberg, R. Martínez and O. Sampayo, Phys. Rev. D **71**, 115003 (2005).
- [39] J. A. M. Vermaseren, mat-ph/0010025.
- [40] J. Pumplin, D. R. Stump, J. Huston, H. L. Lai, P. Nadolsky, and W. K. Tung, JHEP **207**, 12 (2002).
- [41] Jens Erler, Paul Langacker, Shoaib Munir and Eduardo Rojas, JHEP **0908**, 17 (2009).

	Vector couplings	Axial-vector couplings
$Z'\bar{c}u$	$-\frac{\mathcal{U}_{12}^* \mathcal{U}_{11} \cos^2 \theta_w}{\sqrt{3 - 12 \sin^2 \theta_w}}$	$\frac{\mathcal{U}_{12}^* \mathcal{U}_{11} \cos^2 \theta_w}{\sqrt{3 - 12 \sin^2 \theta_w}}$
$Z'\bar{t}u$	$-\frac{\mathcal{U}_{13}^* \mathcal{U}_{11} \cos^2 \theta_w}{\sqrt{3 - 12 \sin^2 \theta_w}}$	$\frac{\mathcal{U}_{13}^* \mathcal{U}_{11} \cos^2 \theta_w}{\sqrt{3 - 12 \sin^2 \theta_w}}$
$Z'\bar{t}c$	$-\frac{\mathcal{U}_{13}^* \mathcal{U}_{12} \cos^2 \theta_w}{\sqrt{3 - 12 \sin^2 \theta_w}}$	$\frac{\mathcal{U}_{13}^* \mathcal{U}_{12} \cos^2 \theta_w}{\sqrt{3 - 12 \sin^2 \theta_w}}$
$Z'\bar{d}s$	$-\frac{\mathcal{V}_{12}^* \mathcal{V}_{11} \cos^2 \theta_w}{\sqrt{3 - 12 \sin^2 \theta_w}}$	$\frac{\mathcal{V}_{12}^* \mathcal{V}_{11} \cos^2 \theta_w}{\sqrt{3 - 12 \sin^2 \theta_w}}$
$Z'\bar{b}d$	$-\frac{\mathcal{V}_{13}^* \mathcal{V}_{11} \cos^2 \theta_w}{\sqrt{3 - 12 \sin^2 \theta_w}}$	$\frac{\mathcal{V}_{13}^* \mathcal{V}_{11} \cos^2 \theta_w}{\sqrt{3 - 12 \sin^2 \theta_w}}$
$Z'\bar{b}s$	$-\frac{\mathcal{V}_{13}^* \mathcal{V}_{12} \cos^2 \theta_w}{\sqrt{3 - 12 \sin^2 \theta_w}}$	$\frac{\mathcal{V}_{13}^* \mathcal{V}_{12} \cos^2 \theta_w}{\sqrt{3 - 12 \sin^2 \theta_w}}$

Table 4: The flavor changing vector and axial-vector couplings to quarks (u - and d -type) induced by Z' in the minimal model.